Conformational Analysis, Barriers to Internal Rotation, Vibrational Assignment, and ab Initio Calculations of 3-Fluoro-1-butene

James R. Durig,* Seung Won Hur,† Todor K. Gounev, Fusheng Feng, and Gamil A. Guirgis‡

Department of Chemistry, University of Missouri—Kansas City, Kansas City, Missouri 64110-2499

Received: October 12, 2000; In Final Form: February 14, 2001

The far-infrared spectrum of gaseous 3-fluoro-1-butene, CH_2═$CHC(CH_3)FH$, has been recorded at a resolution of 0.10 cm^{-1}. The asymmetric torsional fundamentals of the most stable form HE (hydrogen atom eclipses the double bond) and the higher energy FE (fluorine atom eclipses the double bond) conformations have been observed at 88.7 and 105.9 cm^{-1}, respectively, each with several excited states falling to lower frequencies. From variable-temperature (−55 to −100 °C) measurements of the infrared spectra of xenon solutions, the enthalpy difference between the HE and FE conformers has been determined to be 87 ± 6 cm^{-1} (250 ± 17 cal/mol). The same determination yields an enthalpy difference of 292 ± 5 cm^{-1} (835 ± 15 cal/mol) between the HE and the least stable ME (methyl group eclipses the double bond) conformer. From these data, the asymmetric torsional potential function governing internal rotation about the C−C bond has been determined. The potential coefficients are $V_1 = -212 \pm 11$, $V_2 = 381 \pm 12$, and $V_3 = 576 \pm 6$ cm^{-1} for the cosine terms and $V_1' = 322 \pm 17$, $V_2' = -214 \pm 10$, and $V_3' = -240 \pm 13$ cm^{-1} for the sine terms. A complete assignment of the vibrational fundamentals observed from the infrared spectra (3200−30 cm^{-1}) of the gas and solid and the Raman spectra (3200−10 cm^{-1}) of all three physical states is proposed. The vibrational data have been compared to the corresponding quantities obtained from MP2/6-31G(d) ab initio calculations. Additionally, complete equilibrium geometries have been determined for the three conformers using the 6-31G(d) and 6-311+G(d,p) basis sets at the RHF and/or MP2 levels. The results are discussed and compared with the corresponding quantities obtained for other similar molecules.

Introduction

The conformational stabilities of the allyl halides (3-halopropenes), CH_2CHCH_2X, have been of interest to chemists for a number of years where only 3-fluoropropene has the cis conformer as the more stable form in the fluid phases.[1] However, MP2/6-311+G(d,p) ab initio calculations predict the gauche conformer as the more stable rotamer so a rather high-level ab initio calculation is needed to obtain the correct prediction for the conformer stability. Replacement of the fluorine atom by either a methyl group or a cyanide group also results in the cis conformer being the more stable form.[2−4] For the 1-butene molecule, CH_2═$CHCH_2CH_3$, the enthalpy difference between the more stable cis conformer and the gauche form is only 64 ± 10 cm^{-1}, which was obtained[4] from a temperature-dependent infrared study of krypton and xenon solutions. This value is consistent with the conformer stability in the vapor state,[3] and the enthalpy difference is expected to be similar to the value in the gas.[5−9] However, the MP2/6-311++G(d,p) ab initio calculations predict[4] the gauche form to be more stable by 178 cm^{-1} (0.49 kcal/mol). Finally, it should be noted that the barrier to internal rotation of the methyl group on propene[10] is 697.5 ± 0.1 cm^{-1} whereas the cis to gauche barriers in 3-fluoropropene[1] and 1-butene[4] are 1117 ± 10 and 835 ± 48 cm^{-1}, respectively. Therefore, we were interested in determining the conformational stability of 3-fluoro-1-butene, CH_2═$CHCH(CH_3)F$, where three possible conformers should be present in the fluid phases. The methyl group should provide some steric hindrance whereas the fluorine atom should give the maximum effect of the electronegativity on the conformer stability.

Therefore, an infrared and Raman spectroscopic investigation including variable-temperature infrared studies of rare gas solution was initiated of 3-fluoro-1-butene to determine the conformational stability. Additionally, we have obtained the harmonic force fields, infrared intensities, Raman activities, depolarization ratios, and vibrational frequencies from MP2/6-31G(d) ab initio calculations with full electron correlation. We have also carried out ab initio calculations with the 6-311+G(d,p) and 6-311+G(2d,2p) basis sets with full electron correlation by the perturbation method to second order[11] to obtain the optimized geometries and conformational stabilities for both conformers. The results of this spectroscopic and theoretical study are reported herein.

Experimental Section

The 3-fluoro-1-butene sample was prepared by fluorination of crotyl alcohol with (diethylamino)sulfur trifluoride.[12] The products were purified by using a low-temperature, low-pressure vacuum fractionation column, and the compound was identified by NMR and mass spectroscopy.

The far-infrared spectrum (Figure 1) of gaseous 3-fluoro-1-butene, from which the torsional transitions were measured, was recorded on a Nicolet model SXV 200 Fourier transform interferometer with the sample contained in a 1 m cell fitted with polyethylene windows. This instrument is equipped with a vacuum bench and liquid-helium-cooled germanium bolom-

* Corresponding author. Phone: 01-816-235-6038. Fax: 01-816-235-5502. E-mail: durigj@umkc.edu.

† Taken in part from the dissertation of S.W.H., which will be submitted to the Department of Chemistry in partial fulfillment of the Ph.D. degree.

‡ Permanent address: Analytical Research and Development Department, Bayer Corp., P.O. Box 118088, Charleston, SC 29423.

10.1021/jp003763h CCC: $20.00
Published on Web 04/06/2001

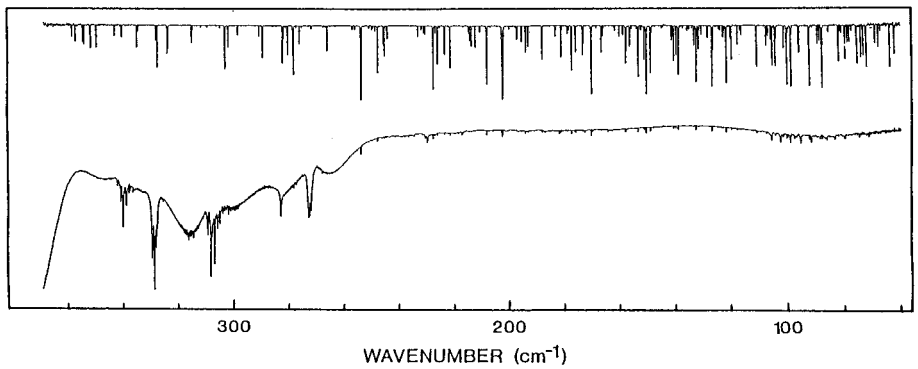

Figure 1. Far-infrared spectrum of gaseous 3-fluoro-1-butene with the top spectrum that of water vapor.

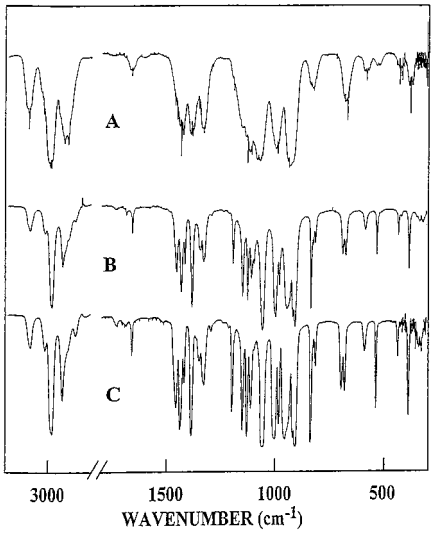

Figure 2. Mid-infrared spectra of 3-fluoro-1-butene in the (A) gas, (B) liquid, and (C) solid phase.

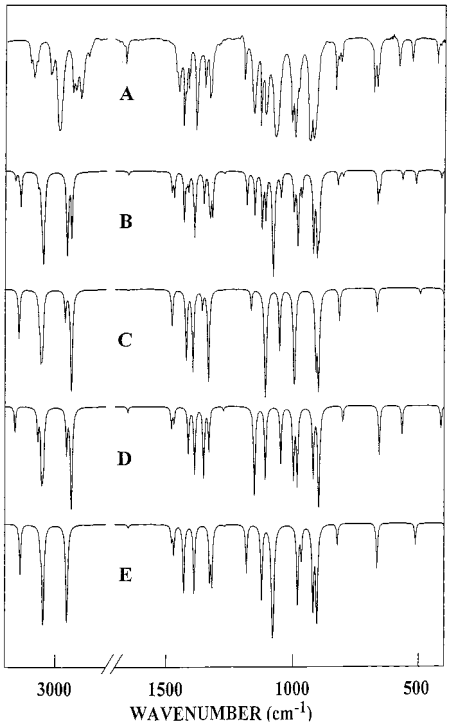

Figure 3. Mid-infrared spectra of 3-fluoro-1-butene: (A) xenon solution at −80 °C; (B) calculated spectrum of the mixture of all three conformers; (C) calculated spectrum of the ME conformer; (D) calculated spectrum of the FE conformer; (E) calculated spectrum of the HE conformer.

eter. The spectrum was collected at a resolution of 0.10 cm^{-1} with 512 interferograms utilizing a 6.25 mm Mylar beam splitter. The far-infrared spectrum of the solid was obtained with a Perkin-Elmer 2000 Fourier transform spectrometer equipped with a solid-state grid beam splitter and a DTGS detector. The sample was deposited onto a silicon plate cooled by boiling liquid nitrogen and housed in a cell fitted with polyethylene windows. After several cycles of warming and cooling the spectrum was recorded.

The mid-infrared spectra of the gas and solid (Figure 2) were recorded on a Perkin-Elmer 2000 Fourier transform spectrometer equipped with a Ge/CsI beam splitter and a DTGS detector. For the gaseous sample, a 10 cm cell fitted with CsI windows was employed. The spectrum of the annealed solid was obtained by depositing the sample onto a CsI plate cooled by boiling liquid nitrogen and housed in a cell fitted with CsI windows.

The mid-infrared spectra of the sample dissolved in liquified xenon (Figure 3A) as a function of temperature were recorded on a Bruker model IFS-66 Fourier Transform interferometer equipped with a Globar source, a Ge/KBr beam splitter, and a DTGS detector. The temperature studies ranged from −55 to −100 °C and were performed in a specially designed cryostat cell consisting of a 4 cm path length copper cell with wedged silicon windows sealed to the cell with indium gaskets. The complete system is attached to a pressure manifold to allow for the filling and evacuation of the cell. The cell is cooled by boiling liquid nitrogen, and the temperature is monitored by two Pt thermoresistors. Once the cell is cooled to the desired temperature, a small amount of sample is condensed into the cell. The system is then pressurized with xenon gas, which immediately starts to condense, allowing the compound to dissolve. For each temperature investigated, 100 interferograms were recorded at 1.0 cm^{-1} resolution, averaged, and transformed with a boxcar truncation function.

The Raman spectra (Figure 4) were recorded on a Cary model 82 spectrophotometer equipped with a Spectra-Physics model 171 argon ion laser operating on the 5145 Å line. The Raman spectrum of the gas was recorded by using a standard Cary multipass accessory. The spectrum of the liquid was obtained from the sample sealed in a Pyrex capillary. The spectrum of the annealed solid was recorded by using a Cryogenic Technology, Inc., cryostat model 20/70 and a model DTC-500 cryogenic temperature controller by Lake Shore Cryogenics, Inc. Reported frequencies are expected to be accurate to at least ±2 cm^{-1}. All observed Raman and infrared bands with significant intensities are listed in Table 1S (Supporting Information).

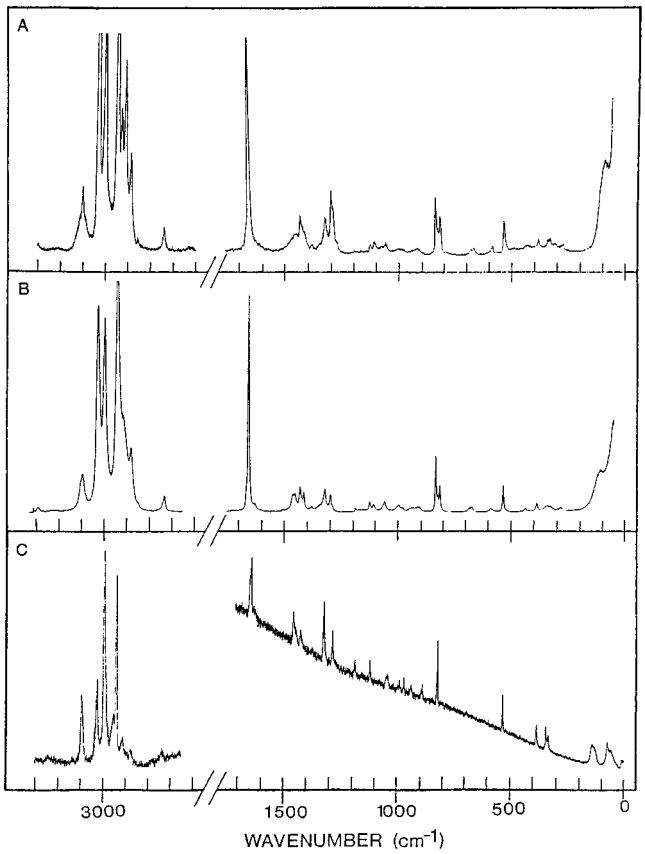

Figure 4. Raman spectra of 3-fluoro-1-butene in the (A) gas, (B) liquid at ambient temperature, and (C) annealed solid phase.

Ab Initio Calculations

The LCAO−MO−SCF restricted Hartree−Fock calculations were performed with the Gaussian-94 program[13] using Gaussian type basis functions. The energy minima with respect to the nuclear coordinates were obtained by the simultaneous relaxation of all of the geometric parameters using the gradient method of Pulay.[14] The calculated structural parameters as determined with the 6-31G(d) and 6-311+G(d,p) basis sets are given in Table 1 for all three conformers. The smaller basis set predicts the FE conformer (fluorine atom eclipsing the double bond) as most stable at both the RHF and MP2 levels; however, the larger basis set favors the HE conformation (hydrogen atom eclipsing the double bond). The least stable form is consistently predicted to be the ME rotamer (methyl group eclipsing the double bond). The torsional potential function (Figure 5) was obtained with the MP2/6-311+G(d,p) calculation by full geometry optimization at the three transition states as well as the three stable potential minima and a subsequent fit of the energies to an asymmetric potential of the type

$$V(\theta) = \sum_{i=1}^{2}\left(\frac{V_i}{2}\right)(1 - \cos i\theta) + \sum_{i=1}^{3}\left(\frac{V_{i'}}{2}\right)\sin i\phi$$

where ϕ is the torsional dihedral angle.

To obtain a more complete description of the molecular motions involved in the normal modes of 3-fluoro-1-butene we have carried out a normal coordinate analysis. The force fields in Cartesian coordinates were calculated by the Gausian-94 program[13] with the MP2/6-31G(d) basis set. Internal coordinates (Figure 6) were used to calculate the *G* and *B* matrixes using the structural parameters given in Table 1. Using the *B* matrix,[15] the force fields in Cartesian coordinates was then converted to a force field in internal coordinates,[16] and the pure ab initio vibrational frequencies were reproduced. The force constants for the three conformers can be obtained from the authors. Subsequently, scaling factors of 0.9 for stretching and bending and 1.0 for the torsional coordinates and the geometric average of scaling factors for interaction force constants were used to obtain the fixed scaled force field and resultant wavenumbers. A set of local symmetry coordinates for various subgroups was used (Table 2S) to determine the corresponding potential energy distributions (PED). A comparison between the observed and calculated frequencies of the three rotamers of 3-fluoro-1-butene along with the calculated infrared intensities, Raman activities, depolarization ratios, and PED are given in Tables 2−4.

To aid the vibrational assignment theoretical infrared (Figure 3) spectra were calculated using fixed scaled wavenumbers and infrared intensities determined from the MP2/6-31G(d) calculation. Infrared intensities were calculated on the basis of the dipole moment derivatives with respect to the Cartesian coordinates. The derivatives were taken from the ab initio calculations and transformed to normal coordinates by

$$\left(\frac{\partial\mu_u}{\partial Q_i}\right) = \sum_j \left(\frac{\partial\mu_u}{\partial X_j}\right)L_{ij}$$

where Q_i is the *i*th normal coordinate, X_j is the *j*th Cartesian displacement coordinate, and L_{ij} is the transformation matrix between the Cartesian displacement coordinates and normal coordinates. The infrared intensities were then calculated by

$$I_i = \frac{N\pi}{3c^2}\left[\left(\frac{\partial\mu_x}{\partial Q_i}\right)^2 + \left(\frac{\partial\mu_y}{\partial Q_i}\right)^2 + \left(\frac{\partial\mu_z}{\partial Q_i}\right)^2\right]$$

The predicted infrared spectra of the ME, FE, and HE conformers are shown in Figure 3C−E, respectively, with the mixture of the two conformers shown in Figure 3B using the experimentally determined ΔH values determined from the variable-temperature studies of the infrared spectra from the liquified xenon solutions. The calculated spectrum is in reasonably good agreement with the mid-infrared spectrum of the sample dissolved in liquid xenon (Figure 3A). Of particular interest are the bands in the spectral region 400−850 cm^{-1} where the individual conformer modes can be confidently assigned.

To aid in the vibrational assignment for each of the conformers, we also simulated the Raman spectra for each conformer. The Raman scattering activities were obtained from the output of the ab initio calculations. The Raman scattering cross sections, $\partial\sigma_j/\partial\Omega$, which are proportional to the Raman intensities, can be calculated from the scattering activities and the predicted wavenumbers for each normal mode.[17−20] To obtain the polarized Raman cross sections, the polarizabilities are incorporated into S_j by $S_j[1 - \rho_j/1 + \rho_j)]$, where ρ_j is the depolarization ratio of the *j*th normal mode. The Raman scattering cross sections and the predicted scaled wavenumbers were used together with a Lorentzian function to obtain the calculated spectra.

The predicted Raman spectrum of the pure HE conformer is shown in Figure 7E, that of pure FE conformer in Figure 7D, and that of the pure ME conformer in Figure 7C. The predicted Raman spectrum of the mixture of the three conformers, with an enthalpy difference of 87 cm^{-1} between the HE and FE and 292 cm^{-1} between the HE and ME conformers with the HE conformer the more stable form, is shown in Figure 7B. This

TABLE 1: Structural Parameters, Rotational Constants, Dipole Moments, and Total Energies for 3-Fluoro-1-butene[a]

	RHF/6 31G(d)			MP2/6 31G(d)			MP2/6 311+G(d,p)		
	HE	FE	ME	HE	FE	ME	HE	FE	ME
r(C═C)	1.317	1.317	1.317	1.336	1.335	1.336	1.339	1.338	1.340
r(C_2–C_3)	1.500	1.502	1.504	1.493	1.497	1.498	1.494	1.498	1.499
r(CF)	1.381	1.375	1.382	1.410	1.403	1.411	1.407	1.398	1.408
r(C_3–C_5)	1.518	1.519	1.515	1.514	1.516	1.511	1.515	1.517	1.512
r(CH_6)	1.083	1.085	1.085	1.096	1.098	1.098	1.095	1.097	1.096
r(CH_7)	1.077	1.074	1.075	1.086	1.083	1.085	1.086	1.084	1.085
r(CH_8)	1.075	1.075	1.075	1.085	1.084	1.085	1.085	1.084	1.085
r(CH_9)	1.078	1.079	1.078	1.089	1.089	1.088	1.089	1.089	1.088
r(CH_{10})	1.084	1.084	1.084	1.092	1.092	1.092	1.092	1.092	1.092
r(CH_{11})	1.084	1.085	1.084	1.093	1.093	1.092	1.093	1.093	1.093
r(CH_{12})	1.085	1.084	1.084	1.093	1.092	1.092	1.093	1.093	1.092
∠(CC═C)	124.3	124.9	126.7	123.5	123.8	125.8	123.1	124.5	125.5
∠($F_4C_3C_2$)	108.2	109.8	107.2	108.1	109.7	107.0	108.4	110.0	107.2
∠($C_5C_3C_2$)	113.2	112.9	116.4	113.1	112.6	116.0	113.0	112.4	115.9
∠($H_6C_3C_2$)	110.2	109.4	109.0	110.2	110.0	109.6	110.0	109.6	109.3
∠($F_4C_3C_5$)	107.6	108.1	108.0	107.4	107.7	107.7	107.8	108.2	108.1
∠($F_4C_3H_6$)	107.0	106.6	105.8	107.0	106.5	105.8	106.5	106.2	105.5
∠($C_5C_3H_6$)	110.5	109.8	109.9	110.8	110.2	110.2	110.9	110.2	110.2
∠(H_7C═C)	121.9	121.7	122.8	121.5	121.1	122.5	121.0	121.1	122.2
∠(H_8C═C)	121.7	121.2	121.0	121.9	121.3	121.0	121.5	120.7	120.7
−(H_9C═C)	120.5	120.3	119.7	120.8	120.7	120.0	120.8	120.4	120.0
∠(H_{10}CC)	110.1	110.1	109.3	110.1	110.2	109.3	110.2	110.2	109.4
∠(H_{11}CC)	110.5	110.7	111.0	110.4	110.7	111.1	109.8	110.1	110.4
∠(H_{12}CC)	110.4	110.0	110.6	109.8	109.3	110.0	110.0	109.7	110.3
∠($H_{10}CH_{11}$)	108.9	108.5	108.3	109.1	108.8	108.5	109.0	108.8	108.4
∠($H_{10}CH_{12}$)	108.3	108.8	108.6	108.6	109.1	108.9	108.8	109.2	109.0
∠($H_{11}CH_{12}$)	108.6	108.6	109.0	108.8	108.8	109.1	108.8	108.8	109.2
τ(FCC═C)	−127.4	1.9	138.2	−125.8	2.4	137.1	−123.0	3.2	136.0
$\|\mu_a\|$	1.025	0.094	1.289	1.126	0.092	1.433	1.166	0.169	1.166
$\|\mu_b\|$	1.643	1.733	1.149	1.759	1.840	1.191	1.974	2.054	1.974
$\|\mu_c\|$	0.327	0.487	0.824	0.342	0.490	0.874	0.432	0.553	0.432
$\|\mu_t\|$	1.963	1.802	1.913	2.117	1.906	2.058	2.333	2.133	2.282
A	8395	8259	8100	8265	8070	8032	8232	8045	8004
B	3623	4069	3985	3599	4092	3960	3602	4071	3967
C	2843	3069	2899	2823	3071	2890	2824	3055	2893
−(E + 254)	0.958 83 6	0.959 42 0	0.957 17 0	1.662 15 8	1.663 17 8	1.660 72 2	1.917 38 5	1.916 88 7	1.915 76 4
ΔE (cm^{-1})	128	0	494	224	0	539	0	109	356

[a] Bond lengths in Å, bond angles in deg, rotational constants in MHz, energies in hartrees, and dipole moments in D.

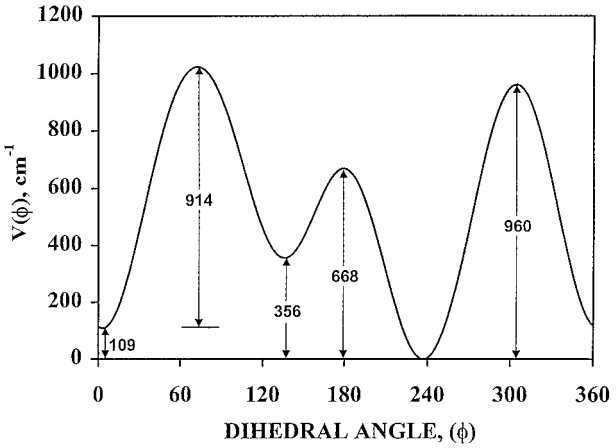

Figure 5. Potential function governing internal rotation of 3-fluoro-1-butene as determined by ab initio calculations with the 6-311+G-(d,p) basis set.

result is considered satisfactory when compared to the experimental Raman spectrum (Figure 7A) of the liquid. The major differences are the three lines at 832, 531, and 383 cm^{-1}, which are much more intense than the predicted Raman intensities. The remaining predicted lines in the region of 100−1500 cm^{-1} showed very good correspondence with the experimental spectrum in both intensities and position, for the most part. Thus, these spectra were quite useful for making the assignments for several of the fundamentals of the less stable conformers.

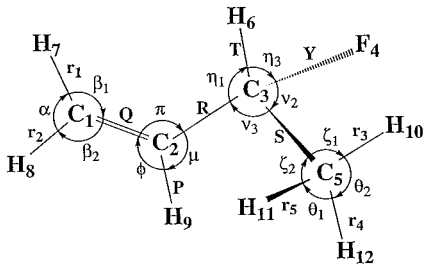

Figure 6. Internal coordinates for 3-fluoro-1-butene.

Conformational Stability

After repeated annealing attempts, the sample of 3-fluoro-1-butene did not produce a polycrystalline solid on the CsI substrate. Therefore, the reported infrared wavenumbers in Table 1S for the solid phase correspond to the amorphous solid where almost all fundamentals from the gas and liquid phases are still present. However, the annealing process in the Pyrex capillary using the Cryogenic Technology, Inc., cryostat was successful and provided clear evidence for the existence of different conformers in the fluid phases but a single conformer in the solid. For example, in the 800 cm^{-1} range (Figure 8), there are three bands associated with the CCC symmetric stretching mode. These bands are evident in the Raman spectra of the gas (Figure 8A) and liquid (Figure 8B) as well as in the infrared spectra of the sample dissolved in liquid xenon (Figure 3A) and the neat liquid (Figure 2B). Upon annealing, only the high-frequency band at 825 cm^{-1} remains in the Raman spectrum of the

TABLE 2: Observed and Calculated Wavenumbers (cm^{-1}) for the Conformer with the Hydrogen Atom Eclipsing the Double Bond (HE) of 3-Fluoro-1-butene

vib no.	fundamental	ab initio[a]	fixed scaled[b]	IR int[c]	Raman act.[d]	dp ratio	obsd[e]	PED
ν_1	$=CH_2$ antisym stretch	3308	3139	10.3	67.4	0.60	3097	$98S_1$
ν_2	=CH stretch	3224	3059	3.7	43.3	0.14	3026	$74S_2$, $22S_5$
ν_3	CH_3 antisym stretch	3214	3049	14.7	70.2	0.73	3001	$90S_3$, $10S_4$
ν_4	CH_3 antisym stretch	3213	3048	21.6	52.0	0.53	2994	$68S_4$, $21S_5$
ν_5	$=CH_2$ sym stretch	3211	3046	1.3	118.0	0.26	2989	$55S_5$, $22S_2$, $21S_4$
ν_6	CH_3 sym stretch	3115	2956	6.7	85.8	0.41	2945	$97S_6$
ν_7	CH stretch	3113	2954	28.2	103.7	0.01	2912	$96S_7$
ν_8	C=C stretch	1737	1648	0.6	30.6	0.18	1657	$67S_8$, $15S_{11}$
ν_9	CH_3 antisym deformation	1559	1479	2.6	17.5	0.74	1458	$69S_9$, $21S_{10}$
ν_{10}	CH_3 antisym deformation	1549	1470	5.3	9.3	0.61	1448	$65S_{10}$, $23S_9$
ν_{11}	$=CH_2$ deformation	1509	1432	16.0	1.3	0.58	1430	$68S_{11}$
ν_{12}	CH_3 sym deformation	1465	1390	16.2	6.5	0.37	1378	$90S_{12}$
ν_{13}	CH bend	1399	1329	11.4	13.8	0.73	1326	$53S_{13}$, $29S_{14}$
ν_{14}	CH bend	1390	1322	13.3	11.4	0.33	1321	$34S_{14}$, $12S_8$, $11S_{11}$, $30S_{13}$
ν_{15}	=CH bend	1339	1272	0.3	16.5	0.57	1286	$57S_{15}$, $10S_8$, $17S_{20}$
ν_{16}	CCC antisym stretch	1247	1192	9.9	3.0	0.49	1189	$17S_{16}$, $10S_{14}$, $13S_{15}$, $12S_{20}$, $12S_{21}$, $13S_{23}$
ν_{17}	CH_3 rock	1184	1131	18.9	3.5	0.70	1125	$36S_{17}$, $21S_{16}$
ν_{18}	CF stretch	1137	1083	67.1	2.1	0.68	1057	$34S_{18}$, $21S_{16}$, $16S_{21}$
ν_{19}	$=CH_2$ twist	1034	981	21.3	1.0	0.71	986	$60S_{19}$, $34S_{24}$
ν_{20}	$=CH_2$ rock	1018	967	6.2	1.4	0.72	981	$33S_{20}$, $11S_{15}$, $23S_{21}$
ν_{21}	CH3 rock	970	919	25.0	10.5	0.66	932	$19S_{21}$, $13S_{16}$, $17S_{17}$, $35S_{18}$
ν_{22}	$=CH_2$ wag	954	905	34.4	3.9	0.73	909	$98S_{22}$
ν_{23}	CCC sym stretch	869	826	3.7	7.5	0.13	833	$42S_{23}$, $14S_{17}$, $11S_{18}$, $16S_{20}$
ν_{24}	=CH bend	700	671	9.0	5.7	0.74	680	$41S_{24}$, $29S_{19}$
ν_{25}	CF bend	540	522	3.6	3.3	0.12	530	$36S_{25}$, $17S_{23}$, $20S_{27}$
ν_{26}	CF bend	381	378	6.2	2.2	0.68	381	$77S_{26}$
ν_{27}	C=CC bend	338	331	1.2	4.8	0.72	330	$47S_{27}$, $30S_{28}$
ν_{28}	CCC bend	313	309	2.7	0.2	0.64	308	$31S_{28}$, $31S_{25}$
ν_{29}	CH_3 torsion	256	255	0.4	2.4	0.65	230	$82S_{29}$
ν_{30}	asym torsion	95	94	0.1	8.1	0.75	89	$89S_{30}$

[a] Calculated using the MP2/6-31G* basis set. [b] Scaled ab initio calculations with factors of 0.9 for stretches and bends and 1.0 for torsions. [c] Calculated intensities in km/mol using the MP2/6-31G* basis set. [d] Calculated Raman activities in $Å^4$/amu using the RHF/3-21G* basis set. [e] Frequencies are taken from the infrared spectrum of the gas, except the ones in parentheses, which are taken from the infrared spectrum of the liquid or sample dissolved in liquid xenon.

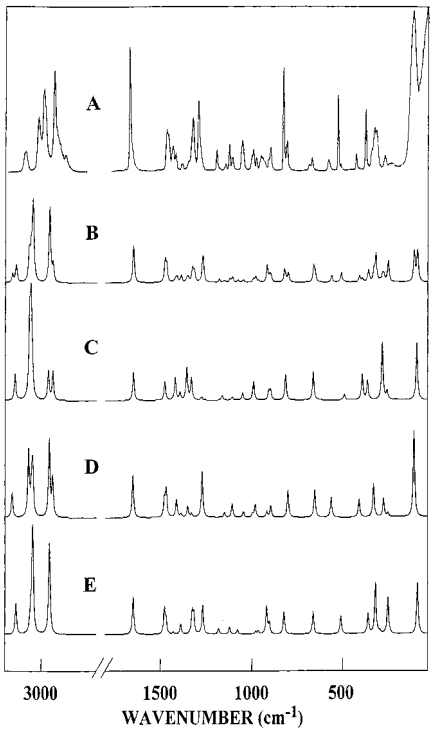

Figure 7. Raman spectra of 3-fluoro-1-butene: (A) experimental spectrum of the liquid at low temperature; (B) calculated spectrum of the mixture of all three conformers; (C) calculated spectrum of ME conformer; (D) calculated spectrum of FE conformer; (E) calculated spectrum of HE conformer.

crystalline solid. This band is assigned to the HE conformer (Table 2), whereas the other two bands are attributed to the ME and FE conformers. Similarly, the bands at 581, 431, and 279 cm^{-1} in the Raman spectrum of the liquid which are confidently assigned to various fundamentals of the FE form (Table 3) and the band at 284 cm^{-1} in the Raman spectrum of the gas which is assigned to the ME rotamer (Table 4) are all absent from the spectrum of the annealed solid. The observed spectral changes are consistent with an equilibrium between three conformations in the fluid phases and a single conformation (HE) present in the crystalline solid.

The above-mentioned conformer bands are sufficiently well separated in the infrared spectrum of the xenon solution and can be used to determine the enthalpy differences, ΔH, between the conformers through temperature-dependent measurements. The ΔH values obtained in this way are a good estimate for the conformational stability of the molecule in the gas phase, since the molar volumes of the conformers are nearly the same.[5-9] The spectra were recorded at 10 different temperatures between -55 and -100 °C (Figure 9). The intensities of six conformer bands at 831, 529 (HE), 811, 582, 428 (FE), and 821 (ME) cm^{-1} were measured, and their ratios were determined (Table 5). By application of the van't Hoff equation, $-\ln K = (\Delta H/RT) - (\Delta S/R)$, where ΔS is the entropy change, the ΔH value was determined by making a plot of $-\ln K$ versus $1/T$, where $\Delta H/R$ is the slope of the line and K is replaced by the appropriate intensity ratio. It is assumed that ΔH is not a function of temperature over this relatively small range. Using a least-squares fit and the slope of the van't Hoff plots, the statistical weighted average ΔH values of 87 ± 6 cm^{-1} (250 ± 17 cal/mol) between the HE and FE conformers and 292 ± 5 cm^{-1} (835 ± 15 cal/mol) between the HE and ME conformers were obtained with the HE form being the most stable conformer.

Vibrational Assignment

The assignment of the fundamentals in the CH stretching and deformation regions (Table 1S) are essentially the same as the

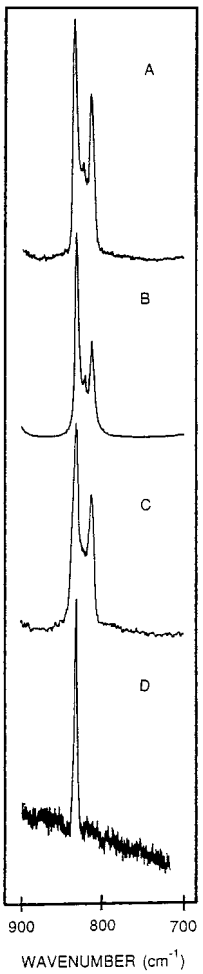

Figure 8. Raman spectrum of 3-fluoro-1-butene in the region of the CCC symmetric stretch: (A) gas; (B) liquid; (C) amorphous solid; (D) annealed solid.

recently proposed assignments for the equivalent molecule of 3-chloro-1-butene.[17] An exception is the CH stretching mode of the hydrogen atom adjacent to the fluorine atom which appears at the lower frequency of ~2910 cm^{-1} than the same mode in the chlorine analogue (2965 cm^{-1}). In addition, the band at ~1410 cm^{-1} can no longer be attributed to an overtone in Fermi resonance but rather to the $=CH_2$ deformations of the high-energy conformers since it is not present in the Raman spectrum of the annealed solid.

The two CH bending modes of the HE conformer are almost degenerate and appear as Q-branches at 1326 and 1321 cm^{-1} in the infrared spectrum of the gas. The band at 1342 cm^{-1} in the infrared spectrum of the xenon solution is assigned to the same mode of the FE rotamer. The =CH bending in the plane of the double bond produces fundamentals at 1297 and 1288 cm^{-1} in the Raman spectrum of the gas for the FE and HE conformers, respectively. The corresponding "out-of-plane" vibration is associated with the series of Q-branches in the 600 cm^{-1} region.

There is extensive mixing of the fundamentals in the 1200−900 cm^{-1} region. For the HE conformer, the highest frequency band in this region at 1191 cm^{-1} is assigned to the CCC antisymmetric stretch although it has significant contributions from several other vibrations. The two CH_3 rocks are assigned to the Q-branches at 1125 and 932 cm^{-1} in the infrared spectrum of the gas, whereas the CF stretch is assigned to the double Q-branch at 1055/1057 cm^{-1}. However, the last two assignments are rather optional and can be reversed since the band at 932 cm^{-1} has ~35% contribution from the CF stretch (Table 2). This, in fact, is also the case with the FE rotamer, where the CF stretch is observed at a lower frequency (927 cm^{-1}) than the CH_3 rock (1061 cm^{-1}) in the spectrum of the xenon solution. The CH_2 twist and rock have approximately the same locations as those of 3-chloro-1-butene[21] and produce very strong bands at 993 and 975 cm^{-1} in the infrared spectra of the condensed phases. The doublet at about 900 cm^{-1} in the same spectrum is due to an almost pure $=CH_2$ wag (98%). The CCC symmetric stretches of the three conformers are clearly resolved and were mentioned earlier.

The heavy atom bending modes exhibit the greatest wavenumber differences among the three conformations. For the HE form, there are two bands at 534 and 385 cm^{-1} in the Raman spectrum of the solid associated with the CF bendings. The respective fundamentals of the FE rotamer are present only in the fluid phases at 582 and 428 cm^{-1} (in liquid xenon), and that of the ME form produces the weak feature at 417 cm^{-1} in the infrared spectrum of the liquid. The doublet at 342/332 cm^{-1} in the Raman spectrum of the solid is attributed to a solid-state splitting of the C=CC bending fundamental of the HE conformer, whereas the similar doublet (346/333 cm^{-1}) in the spectrum of the liquid is interpreted as two conformer bands with the high-frequency component assigned to the CCC bend of the FE form.

A series of A-type Q-branches in the far-infrared spectrum of the gas starting at 310 cm^{-1} is assigned to the CCC bend of the HE rotamer having the equivalent mode of the ME form as a well-defined C-type band at 283 cm^{-1}. The nearby Q-branch at 273 cm^{-1} is actually a part of an A-type band assigned to the C=CC bend of the FE conformer. The methyl torsions are also observed in the far-infrared spectrum of the gas (Figure 10) at 230 cm^{-1}, whereas the asymmetric torsional mode gives rise to two sets of pronounced Q-branches (Figure 11) starting at 106 and 89 cm^{-1} assigned to the FE and HE conformers, respectively.

Discussion

The potential function of the asymmetric rotor can be calculated using the far-infrared transitions assigned to the torsional modes and the respective "hot" bands of the modes for the different conformers. The observed transitions and their assignments are listed in Table 6. The FE conformer produces the stronger series of Q-branches (Figure 11) starting at 105.8 cm^{-1} as expected from the ab initio calculations (Tables 2−4), whereas the lower frequency series starting at 88.7 cm^{-1} is assigned to the HE form. There are several other less prominent Q-branches in this spectral region that can be assigned to the transitions of the ME rotamer. However, these less intense bands could also be attributed to excited states of the low-frequency bending modes arising from the same HE and FE forms. Thus, transitions of the ME conformer were not used in the fit of the potential function. Using the 10 far-infrared transitions and the two ΔH values from the temperature study of the xenon solution spectra, a potential function was obtained of the type described earlier having three cosine and three sine coefficients. The potential coefficients as well as the resulting barriers to internal rotation are listed in Table 7 and compared to the values obtained from ab initio calculations at the MP2/6-311+G(d,p) level. The actual function is shown in Figure 12, where the calculated energy levels and observed transitions are also depicted. The states lying above the ME-to-HE barrier appear in progressively separating pairs that correspond to a wide amplitude torsional oscillation. The fundamental transition of

TABLE 3: Observed and Calculated Wavenumbers (cm^{-1}) for the Conformer with the Fluorine Atom Eclipsing the Double Bond (FE) of 3-Fluoro-1-butene

vib no.	fundamental	ab initio[a]	fixed scaled[b]	IR int[c]	Raman act.[d]	dp ratio	obsd[e]	PED
ν_1	$=CH_2$ antisym stretch	3330	3160	4.5	55.1	0.74	3112	$99S_1$
ν_2	=CH stretch	3216	3050	12.5	64.0	0.67		$71S_2$, $12S_3$, $12S_5$
ν_3	CH3 antisym stretch	3220	3055	16.4	37.4	0.71		$56S_3$,$43S_4$
ν_4	CH_3 antisym stretch	3210	3046	7.0	63.3	0.71		$53S_4$, $13S_2$, $33S_3$
ν_5	$=CH_2$ sym stretch	3237	3070	5.5	135.8	0.13	3032	$85S_5$, $14S_2$
ν_6	CH_3 sym stretch	3116	2956	9.1	152.7	0.25	2929	$100S_6$
ν_7	CH stretch	3096	2937	36.7	74.9	0.04		$99S_7$
ν_8	C=C stretch	1739	1651	1.0	34.8	0.20		$68S_8$, $14S_{11}$
ν_9	CH_3 antisym deformation	1560	1480	3.7	12.6	0.75	1462	$66S_9$, $24S_{10}$
ν_{10}	CH_3 antisym deformation	1550	1470	2.8	19.3	0.73	1450	$64S_{10}$, $25S_9$
ν_{11}	$=CH_2$ deformation	1491	1415	9.2	12.1	0.42	1410	$76S_{11}$
ν_{12}	CH_3 sym deformation	1464	1390	15.4	2.2	0.41	1378	$91S_{12}$
ν_{13}	CH bend	1426	1357	16.8	6.8	0.73	1348	$72S_{13}$
ν_{14}	CH bend	1404	1333	8.6	2.2	0.74		$65S_{14}$
ν_{15}	=CH bend	1343	1275	0.7	26.4	0.40	1293	$58S_{15}$, $14S_8$, $14S_{20}$
ν_{16}	CCC antisym stretch	1169	1116	17.9	6.7	0.38	1107	$18S_{16}$, $19S_{17}$, $10S_{21}$, $20S_{23}$
ν_{17}	CH_3 rock	1214	1158	25.8	2.4	0.73	(1147)	$16S_{17}$, $14S_{13}$, $23S_{18}$, $11S_{25}$
ν_{18}	CF stretch	970	919	17.0	2.2	0.75	931	$29S_{18}$, $18S_{16}$, $20S_{17}$, $20S_{21}$
ν_{19}	$=CH_2$ twist	1036	983	20.9	5.3	0.72	986	$64S_{19}$, $25S_{24}$
ν_{20}	$=CH_2$ rock	1052	999	17.6	1.6	0.74	1007	$38S_{20}$, $17S_{15}$, $11S_{16}$, $12S_{18}$
ν_{21}	CH_3 rock	1105	1054	12.3	2.7	0.68	(1061)	$28S_{21}$, $14S_{14}$, $13S_{16}$, $12S_{20}$
ν_{22}	$=CH_2$ wag	947	898	35.8	4.3	0.75	909	$98S_{22}$
ν_{23}	CCC sym stretch	846	804	2.7	8.8	0.23	812	$48S_{23}$, $11S_{17}$, $13S_{18}$, $10S_{21}$
ν_{24}	=CH bend	692	661	10.0	6.8	0.53	667	$34S_{24}$, $18S_{19}$, $12S_{23}$, $10S_{28}$
ν_{25}	CF bend	596	581	5.0	4.1	0.55	582	$21S_{25}$, $10S_{24}$, $16S_{26}$, $28S_{27}$
ν_{26}	CF bend	434	426	3.9	2.4	0.63	428	$44S_{26}$, $26S_{25}$
ν_{27}	C=C−C bend	289	287	1.4	1.4	0.70	273	$26S_{27}$, $22S_{25}$, $13S_{28}$, $31S_{29}$
ν_{28}	CCC bend	350	344	1.3	3.3	0.62	340	$49S_{28}$, $16S_{26}$, $10S_{27}$
ν_{29}	CH_3 torsion	258	257	0.8	0.3	0.70		$64S_{29}$, $19S_{27}$
ν_{30}	asym torsion	113	113	0.3	8.0	0.75	106	$88S_{30}$

[a] Calculated using the MP2/6-31G* basis set. [b] Scaled ab initio calculations with factors of 0.9 for stretches and bends and 1.0 for torsions. [c] Calculated intensities in km/mol using the MP2/6-31G* basis set. [d] Calculated Raman activities in $Å^4$/amu using the RHF/3-21G* basis set. [e] Frequencies are taken from the infrared spectrum of the gas, except the ones in parentheses, which are taken from the infrared spectrum of the liquid or sample dissolved in liquid xenon.

ME conformer is predicted to be between the transitions for the HE and FE forms at ~90 cm^{-1}.

There is a great similarity between the ab initio calculated (Figure 5) and experimentally determined (Figure 12) potential functions both in terms of the general shape of the potential surface and the values of the potential coefficients. The barrier between the ME and HE conformers is significantly lower than the other two barriers. This can be explained with a favorable interaction between the fluorine atom and the methylene hydrogen (H9) which eclipse each other in the ME/HE transition state. In contrast, in 3-chloro-1-butene[21] the ME/HE transition state has the highest energy due to the larger size of the chlorine atom eclipsing the methylene hydrogen.

The methyl torsions for the three conformers of 3-fluoro-1-butene are predicted by the ab initio calculations at almost the same frequency (Tables 2−4) in the 200 cm^{-1} region. Two clusters of bands (Figure 10) centered at 230 and 217 cm^{-1} are observed in the far-infrared spectrum of the gas for these modes. From the wavenumber separation between the clusters and their intensity it can be predicted that the higher frequency set of Q-branches are the $1 \leftarrow 0$ transitions of the CH_3 torsions for at least two of the conformers (HE and FE), whereas the lower frequency set is due to the $2 \leftarrow 1$ transitions of the CH_3 torsion. The torsional fundamental of the FE conformer has a predicted infrared intensity twice that of the HE form (Tables 2 and 3), so the stronger Q-branches at 230 and 217 cm^{-1} are tentatively assigned to the methyl torsional modes of the HE form. Using this assignment the barrier to methyl rotation is calculated to be 1226 cm^{-1} utilizing a potential function having two cosine terms, $V_3 = 1226$ cm^{-1} and $V_6 = 11$ cm^{-1}, and an F number ($F = h^2/8\pi^2 c I_r$, where I_r is the reduced moment of internal rotation) of 5.494 376 cm^{-1}. The small value of the V_6 term compared to the V_3 term is consistent with what is usually obtained for methyl barriers and supports the assignment.

The methyl barrier compares well with the barrier value for the gauche conformer of 1-butene[4] (1180 cm^{-1}) but is significantly lower than the value for the cis form (1695 cm^{-1}) of the same molecule where the methyl group eclipses the double bond. However, it should be mentioned that in the ME conformer, the CH_3 group is ~17° away from a totally eclipsed geometry (Table 1). Additionally, the methyl barrier for the ME form may be slightly higher than 1226 cm^{-1} since the frequency of the torsional mode for this conformation is predicted about 10 cm^{-1} higher than the fundamentals of the FE and HE rotamers (Tables 2−4) and several weaker Q-branches are observed between 236 and 240 cm^{-1} (Figure 10).

The structural differences between the conformers of 3-fluoro-1-butene are most significant for the parameters closest to the axis of internal rotation. The bond distances for the C_3–C_5, C−F, and C−H_6 bonds are shorter for the conformations in which these bonds eclipse the double bond. The CCF and $C_5C_3C_2$ bond angles are 2−3° larger for the FE and ME conformers, respectively, whereas the C−C=C bond angle opens by about 1° on conversion from HE to FE to ME conformation. In addition, the asymmetric torsional dihedral angle deviates most from the eclipsed position of the double bond for the ME conformer. A comparison of the structural parameters of 3-fluoro-1-butene and 3-chloro-1-butene[21] calculated with the MP2/6-311+G(d,p) basis set shows them to be essentially the same for the common parts of the two molecules. The double bond distance is not influenced by the substituent; however,

TABLE 4: Observed and Calculated Wavenumbers (cm^{-1}) for the Conformer with the Methyl Group Eclipsing the Double Bond (ME) for 3-Fluoro-1-butene

vib no.	fundamental	ab initio[a]	fixed scaled[b]	IR int[c]	Raman act.[d]	dp ratio	obsd[e]	PED
ν_1	$=CH_2$ antisym stretch	3315	3145	9.9	57.3	0.66	3086	$99S_1$
ν_2	=CH stretch	3232	3066	3.5	155.5	0.19		$50S_2$, $48S_5$
ν_3	CH_3 antisym stretch	3224	3059	13.3	160.2	0.22		$55S_3$, $45S_4$
ν_4	CH_3 antisym stretch	3216	3051	10.6	52.9	0.68		$50S_4$, $42S_3$
ν_5	$=CH_2$ sym stretch	3221	3055	8.9	30.3	0.42		$46S_5$, $46S_2$
ν_6	CH_3 sym stretch	3122	2962	5.4	57.5	0.70		$100S_6$
ν_7	CH stretch	3096	2937	36.7	56.4	0.08		$99S_7$
ν_8	C=C stretch	1737	1649	0.2	22.7	0.18		$67S_8$, $16S_{11}$
ν_9	CH_3 antisym deformation	1559	1479	2.9	9.6	0.70		$57S_9$, $34S_{10}$
ν_{10}	CH_3 antisym deformation	1557	1477	4.5	4.0	0.55		$50S_{10}$, $36S_9$
ν_{11}	$=CH_2$ deformation	1499	1423	16.7	15.0	0.66	1420	$70S_{11}$
ν_{12}	CH_3 sym deformation	1471	1397	22.1	4.6	0.37	1380	$63S_{12}$, $12S_{14}$, $14S_{16}$
ν_{13}	CH bend	1405	1336	28.2	13.3	0.70	(1338)	$78S_{13}$
ν_{14}	CH bend	1433	1362	3.2	20.5	0.41		$46S_{14}$, $27S_{12}$
ν_{15}	=CH bend	1347	1279	0.1	1.9	0.72		$60S_{15}$, $14S_8$, $13S_{20}$
ν_{16}	CCC antisym stretch	1228	1173	3.5	2.5	0.40	1158	$34S_{16}$, $11S_{14}$, $19S_{17}$
ν_{17}	CH_3 rock	1109	1057	13.4	3.1	0.64		$16S_{17}$, $19S_{14}$, $23S_{21}$
ν_{18}	CF stretch	1169	1117	47.4	1.7	0.75	(1093)	$31S_{18}$, $15S_{17}$, $22S_{21}$
ν_{19}	$=CH_2$ twist	1045	993	15.8	6.9	0.74		$62S_{19}$, $32S_{24}$
ν_{20}	$=CH_2$ rock	1050	996	22.2	1.2	0.63	1003	$39S_{20}$, $13S_{15}$, $19S_{18}$, $18S_{23}$
ν_{21}	CH_3 rock	959	910	19.7	3.5	0.75		$24S_{21}$, $15S_{16}$, $13S_{17}$, $31S_{18}$, $12S_{20}$
ν_{22}	$=CH_2$ wag	949	909	37.9	3.7	0.75	(913)	$98S_{22}$
ν_{23}	CCC sym stretch	861	819	5.9	8.4	0.22	823	$44S_{23}$, $16S_{17}$
ν_{24}	=CH bend	701	669	4.1	7.1	0.45	678	$29S_{24}$, $21S_{19}$, $18S_{23}$
ν_{25}	CF bend	417	409	5.0	3.2	0.64	(417)	$55S_{25}$, $19S_{26}$
ν_{26}	CF bend	386	379	1.0	2.2	0.66		$53S_{26}$, $12S_{24}$, $12S_{28}$
ν_{27}	C=C−C bend	521	509	0.9	1.0	0.53	(510)	$39S_{27}$, $23S_{28}$
ν_{28}	CCC bend	268	291	1.2	0.6	0.63	283	$31S_{28}$, $28S_{27}$, $31S_{29}$
ν_{29}	CH_3 torsion	293	266	0.9	4.5	0.70		$66S_{29}$, $11S_{27}$, $12S_{28}$
ν_{30}	asym torsion	99	98	0.5	8.1	0.75		$94S_{30}$

[a] Calculated using the MP2/6-31G* basis set. [b] Scaled ab initio calculations with factors of 0.9 for stretches and bends and 1.0 for torsions. [c] Calculated intensities in km/mol using the MP2/6-31G* basis set. [d] Calculated Raman activities in $Å^4$/amu using the RHF/3-21G* basis set. [e] Frequencies are taken from the infrared spectrum of the gas, except the ones in parentheses, which are taken from the infrared spectrum of the liquid or sample dissolved in liquid xenon.

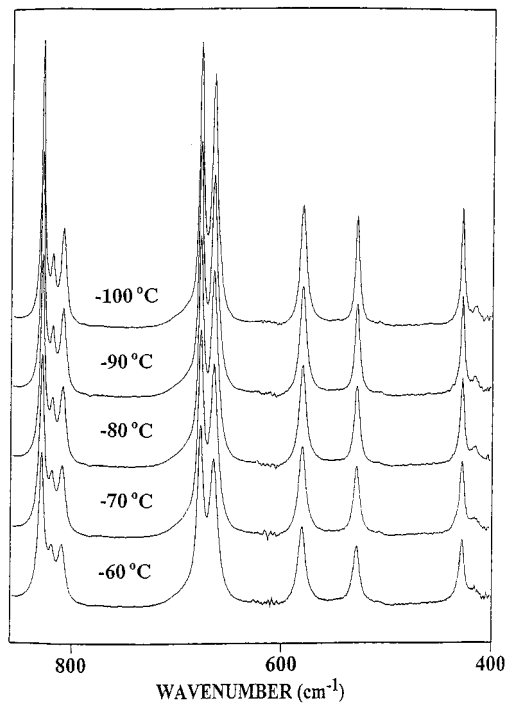

Figure 9. Temperature-dependent infrared spectrum (860−400 cm^{-1}) of 3-fluoro-1-butene in liquid xenon.

the C_3–C_5 distance is about 0.005 Å shorter for all conformers of the fluorine compound.

As opposed to the case of 3-chloro-1-butene,[21] where the calculated ab initio energy differences between the conformers were grossly overestimated compared to the experimental enthalpy values, the predicted ab initio energy differences (Table 2) for 3-fluoro-1-butene have more realistic values. However, this is achieved only with the relatively large basis set (MP2/6-311+G(d,p)). The smaller basis sets (Table 1) incorrectly predict the FE conformer to be more stable than the HE form.

To test whether even larger basis sets can improve the prediction of the conformational energy difference, we calculated the energies of the three conformers using the MP2/6-311++G-(3df,3pd) basis set retaining the MP2/6-311+G(d,p) geometry. The resulting energy differences actually dropped below the experimental values to 6 and 200 cm^{-1} for the HE/FE and HE/ME conformer pairs, respectively. These large variations in the calculated energies shows that for the above-mentioned two molecules, ab initio calculations performed with "standard" basis sets, i.e., 6-31G(d), at the RHF and MP2 levels cannot be used as reliable estimates of the conformational stability without experimental verification. The same conclusion was reached in the theoretical studies of the similar molecules 3-fluoropropene[1] and 1-butene.[4]

From the excellent agreement of the predicted infrared spectra with the infrared spectra of the sample dissolved in liquid xenon it can be concluded that the utilized experimental ΔH values are reasonably well determined. Only minor discrepancies are encountered between the observed and calculated spectra. These are primarily due to wavenumber inconsistencies such as the observation of nearly coincident CF stretching and CH_3 rocking modes for the HE and FE conformers, respectively, as opposed to the prediction that the two bands are separated at 1083 and 1054 cm^{-1}.

It is interesting to note that the enthalpy differences between the HE and ME conformers of 3-chloro-[21] and 3-fluoro-1-butene

TABLE 5: Temperature and Intensity Ratio for the Conformational Stability Study of 3-Fluoro-1-butene in Liquid Xenon

T (°C)	T (K)	1000/T (K)	I_{821}(ME)/I_{83}(HE)	$-\ln K$	I_{821}(ME)/I_{529}(HE)	$-\ln K$
−55	218	4.587	0.405	0.903	1.053	0.052
−60	213	4.695	0.378	0.973	0.980	0.020
−65	208	4.808	0.366	1.006	0.942	0.060
−70	203	4.926	0.344	1.066	0.916	0.088
−75	198	5.051	0.327	1.119	0.864	0.146
−80	193	5.181	0.310	1.171	0.826	0.191
−85	188	5.319	0.295	1.222	0.788	0.238
−90	183	5.464	0.276	1.288	0.735	0.308
−95	178	5.618	0.260	1.346	0.681	0.384
−100	173	5.780	0.242	1.419	0.618	0.481
$^{\Delta}H^{a}$ (cm^{-1})				293 ± **4**		291 ± **10**

T (°C)	T (K)	1000/T (K)	I_{811}(FE)/I_{831}(HE)	$-\ln K$	I_{582}(FE)/I_{831}(HE)	$-\ln K$	I_{428}(FE)/I_{831}(HE)	$-\ln K$
−55	218	4.587	0.397	0.923	0.511	0.671	0.432	0.840
−60	213	4.695	0.389	0.943	0.509	0.676	0.433	0.837
−65	208	4.808	0.386	0.951	0.490	0.712	0.421	0.865
−70	203	4.926	0.381	0.965	0.479	0.735		
−75	198	5.051	0.369	0.997	0.467	0.761	0.417	0.874
−80	193	5.181	0.367	1.001	0.469	0.756	0.420	0.867
−85	188	5.319	0.360	1.021	0.457	0.783		
−90	183	5.464	0.352	1.045	0.438	0.825	0.405	0.903
−95	178	5.618	0.341	1.075	0.438	0.825	0.407	0.899
−100	173	5.780	0.338	1.084	0.411	0.890		
$^{\Delta}H^{b}$ (cm^{-1})				96 ± **3**		119 ± **8**		43 ± **7**

T (°C)	T (K)	1000/T (K)	I_{811}(FE)/I_{529}(HE)	$-\ln K$	I_{582}(FE)/I_{529}(HE)	$-\ln K$	I_{428}(FE)/I_{529}(H E)	$-\ln K$
−55	218	4.587	1.032	0.031	1.328	0.284	1.122	0.115
−60	213	4.695	1.010	0.010	1.319	0.277	1.123	0.116
−65	208	4.808	0.996	0.004	1.263	0.234		
−70	203	4.926	1.013	0.013	1.274	0.242	1.097	0.093
−75	198	5.051	0.977	0.024	1.236	0.212	1.105	0.100
−80	193	5.181	0.978	0.022	1.250	0.223	1.120	0.113
−85	188	5.319	0.963	0.038	1.222	0.201		
−90	183	5.464	0.938	0.064	1.168	0.155	1.081	0.078
−95	178	5.618	0.893	0.114	1.147	0.137	1.065	0.063
−100	173	5.780	0.864	0.146	1.049	0.048	1.064	0.062
ΔH^{b} (cm^{-1})				94 ± 11		117 ± 14		33 ± 6

[a] Average ΔH(ME/HE) = 292 ± 5 cm^{-1} (835 ± 15 cal/mol). [b] Average ΔH(FE/HE) = 87 ± 6 cm^{-1} (250 ± 17 cal/mol).

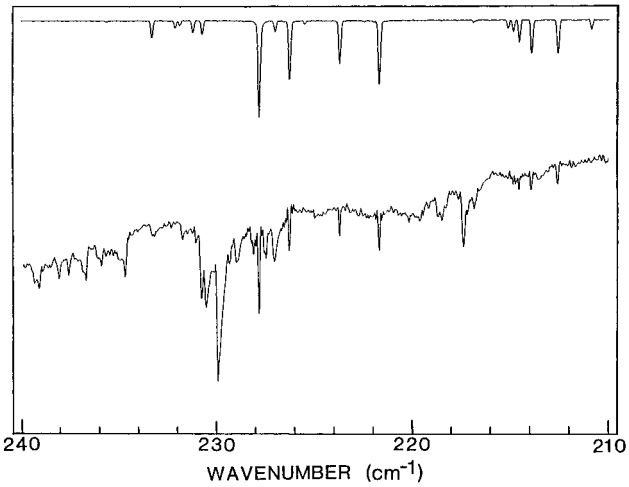

Figure 10. Far-infrared spectrum of gaseous 3-fluoro-1-butene in the region of the methyl group torsion.

are 75 ± 8 and 292 ± 5 cm^{-1}, respectively, which is a rather large difference. This destabilization of the ME conformer for the fluorine compound can be attributed to the shorter C_3–C_5 distance mentioned earlier that brings the methyl group closer to the double bond. On the other hand, the ClE conformer of 3-chloro-1-butene is 197 ± 37 cm^{-1} less stable than the HE form, whereas the equivalent FE conformer of 3-fluoro-1-butene is only 87 ± 6 cm^{-1} above the HE rotamer. This difference is

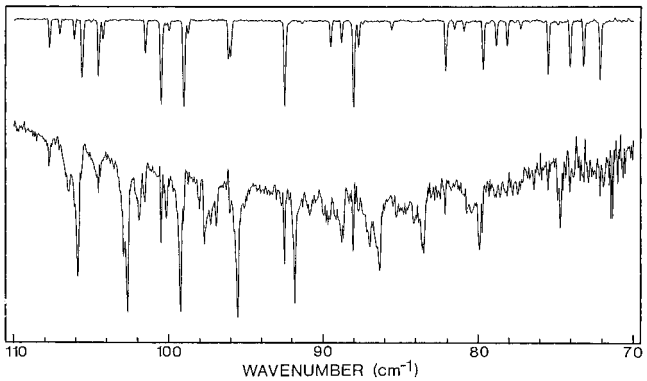

Figure 11. Far-infrared spectrum of gaseous 3-fluoro-1-butene in the region of the asymmetric torsional mode.

logically related to the size of the substituent eclipsing the double bond in the two compounds.

The 3-fluoro-1-butene molecule can be viewed as a result of a substitution of two hydrogen atoms in propene with a fluorine atom and a CH_3 group. The conformational stability of this molecule, therefore, should be also comparable to those of 3-fluoropropene (allyl fluoride) and 1-butene, where either only a fluorine atom or only a methyl group is substituted. The enthalpy differences between the cis and gauche conformers of the latter two compounds have been determined[1,4] in liquid xenon solution to be 60 ± 8 and 64 ± 10 cm^{-1}, respectively, with the cis conformers more stable in both cases. These results

TABLE 6: Far-Infrared Torsional Transitions (cm^{-1}) of Gaseous 3-Fluoro-1-butene

conformer	transn	obsd	calcd[a]	obsd − calcd
FE[b]	1 ← 0	105.879	105.498	0.381
	2 ← 1	102.668	102.563	0.105
	3 ← 2	99.299	99.286	0.013
	4 ← 3	95.560	95.573	−0.013
	5 ← 4	91.892	91.760	0.132
HE[c]	1 ← 0	88.700	88.265	0.435
	2 ← 1	86.400	86.554	−0.154
	3 ← 2	83.509	84.003	−0.524
	4 ← 3	79.965	80.415	−0.450
	5 ← 4	74.700	74.740	−0.040

[a] Calculated using the potential coefficients given in Table 7. [b] FE refers to the conformer in which the fluorine atom eclipses the double bond with C=CCF dihedral angle of $t = 3.2°$. [c] HE refers to the conformer in which the methyl group eclipses the double bond with C=CCF dihedral angle of $t = 237.0°$. [d] ME refers to the conformer in which the hydrogen on the carbon, bonded to the fluorine atoms, eclipses the double bond with C=CCF dihedral angle of $t = 136.0°$.

TABLE 7: Calculated Potential Constants (cm^{-1}), Resultant Barriers (cm^{-1}), and Enthalpy Difference (cm^{-1}) for the Asymmetric Torsion of 3-Fluoro-1-butene

coeff	exptl	ab initio (MP2/ 6-311+G(d,p))	coeff	exptl	ab initio (MP2/ 6-311+G(d,p))
V_1	212 ± 11	158	ΔH(FE/HE) (cm^{-1})	87	109
V_2	381 ± 12	289	ΔH(ME/HE) (cm^{-1})	292	356
V_3	576 ± 6	668	ME/HE barrier	233	312
V_1'	322 ± 17	281	HE/FE barrier	915	960
V_2'	214 ± 10	212	FE/ME barrier	933	914
V_3'	240 ± 13	169			

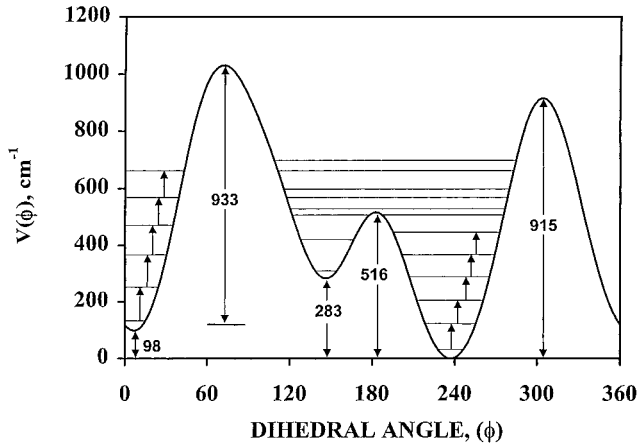

Figure 12. Asymmetric torsional potential function for 3-fluoro-1-butene as determined from far-infrared spectral data. The torsional dihedral angle of 0° corresponds to the conformation in which the fluorine atom is oriented cis to the double bond.

seem strange compared to our results for 3-fluoro-1-butene because the cis conformers of 3-fluoropropene and 1-butene correspond to the FE and ME conformers of 3-fluoro-1-butene, respectively, whereas the gauche conformers correspond to the HE rotamer in our study. If the experimental ΔH values are correct, then obviously the effects of the CH_3 group and the fluorine atom as substituents in 1-butene and 3-fluoropropene offset each other when they are simultaneously substituted in 3-fluoro-1-butene. The enthalpy difference between the FE and HE conformers in our study is quite small, and therefore, one can attribute experimental uncertainty, solute−solvent interactions, or packing effects in the solvent matrix for the difference between the value obtained in this investigation and that of 3-fluoropropene[1] where the ΔH value is also quite small. However, the same explanation cannot be given for the much larger ΔH value between the HE and ME forms (292 ± 5 cm^{-1}). It is not clear why the eclipsed position of the methyl group is 64 ± 10 cm^{-1} more stable in 1-butene,[4] whereas it is 292 ± 5 cm^{-1} less stable in 3-fluoro-1-butene. However, it is expected that the C_2C_3 bond distance may have a pronounced effect on the relative stabilities for these three molecules, particularly since the ab initio MP2/6-311+(d,p) calculations for 3-fluoropropene predicted[1] the gauche conformer to be more stable by 252 cm^{-1}, whereas the experimental results give the cis form more stable by 60 ± 8 cm^{-1}. Therefore, higher level ab initio calculations could be valuable in providing explanations for the relative stabilities of the conformers of 1-butene, 3-fluoropropene, and 3-fluoro-1-butene.

Acknowledgment. J.R.D. acknowledges partial support of these studies by the University of Missouri—Kansas City Faculty Research Grant program.

Supporting Information Available: Table 1S, observed infrared and Raman wavenumbers (cm^{-1}) for 3-fluoro-1-butene, and Table 2S, symmetry coordinates for vibrations of 3-fluoro-1-butene. This material is available free of charge via the Internet at http://pubs.acs.org.

References and Notes

(1) Van der Veken, B. J.; Herrebout, W. A.; Durig, D. T.; Zhao, W.; Durig, J. R. *J. Phys. Chem. A* **1999**, *103*, 1976.

(2) Durig, J. R.; Guirgis, G. A.; Drew, A. S. *J. Raman Spectrosc*. **1994**, *25*, 907.

(3) Gallinella, E.; Cadioli, B. *Vib. Spectrosc*. **1997**, *13*, 163.

(4) Bell, S.; Drew, B. R.; Guirgis, G. A.; Durig, J. R. *J. Mol. Struct*. **2000**, *553*, 199.

(5) Herrebout, W. A.; Van der Veken, B. J. *J. Phys. Chem*. **1996**, *100*, 9671.

(6) Herrebout, W. A.; Van der Veken, B. J.; Wang, A.; Durig, J. R. *J. Phys. Chem*. **1995**, *99*, 578.

(7) Bulanin, M. O. *J. Mol. Struct.* **1973**, *19*, 59.

(8) Van der Veken, B. J.; DeMunck, F. R. *J. Chem. Phys*. **1992**, *97*, 3060.

(9) Bulanin, M. O. *J. Mol. Struct.* **1995**, *347*, 73.

(10) Pearson, J. C.; Sastry, K. V. L. N.; Jlerbst, E.; De Lucia, F. C. *J. Mol. Spectrosc.* **1994**, *166*, 120.

(11) Moller, C.; Plesset, M. S. *Phys. Rev*. **1934**, *46*, 618.

(12) Middleton, W. J. *J. Org. Chem*. **1975**, *40*, 574.

(13) Frisch, M. J.; Trucks, G. W.; Schlegel, H. B.; Gill, P. M. W.; Johnson, B. G.; Robb, M. A.; Cheeseman, J. R.; Keith, T. A.; Petersson, G. A.; Montgomery, J. A.; Raghavachari, K.; Al-Laham, M. A.; Zakrzewski, V. G.; Ortiz, J. V.; Foresman, J. B.; Cioslowski, J.; Stefanov, B. B.; Nanayakkara, A.; Challacombe, M.; Peng, C. Y.; Ayala, P. Y.; Chen, W.; Wong, M. W.; Andres, J. L.; Replogle, E. S.; Gomperts, R.; Martin, R. L.; Fox, D. J.; Binkley, J. S.; Defrees, D. J.; Baker, J.; Stewart, J. P.; Head-Gordon, M.; Gonzalez C.; Pople, J. A. *Gaussian 94*, revision B3; Gaussian Inc.: Pittsburgh, PA, 1995.

(14) Pulay, P. *Mol. Phys*. **1969**, *17*, 197.

(15) Wilson, E. B.; Decius, J. C.; Cross, P. C. *Molecular Vibrations*; McGraw-Hill: New York, 1955 (republished: Dover: New York, 1980).

(16) Schachtschneider, J. H. *Vibrational Analysis of Polyatomic Molecules*; Technical Report Nos. 231 and 57; Shell Development Co.: Houston, TX, 1964 and 1965; Parts V and VI.

(17) Frisch, M. J.; Yamagushi, Y.; Gaw, J. F.; Schaefer III, H. F.; Binkley, J. S. *J. Chem. Phys.* **1986**, *84*, 531.

(18) Amos, R. D. *Chem. Phys. Lett.* **1986**, *124*, 376.

(19) Polavarapu, P. L. *J. Phys. Chem.* **1990**, *94*, 8106.

(20) Chantry, G. W. In *The Raman Effect*; Anderson, A., Ed.; Marcel Dekker Inc.: New York, 1971; Vol. 1, Chapter 2.

(21) Lee, M. J.; Fusheng, F.; Hur, S. W.; Liu, J.; Gounev, T. K.; Durig, J. R.; *J. Raman Spectrosc.* **2000**, *31*, 157.